CDF/ANAL/EXOTIC/PUBLIC/7747
Version 1.0
July 8, 2005

Search for R-Parity Violating Sneutrino Decay in the High Mass $e\mu$ Channel

The CDF Collaboration
http://www-cdf.fnal.gov

Abstract

We present the results of a search for the production and decay the Supersymmeteric partner of the tau neutrino, $\tilde{\nu_\tau}$, in a model that assumes R-parity violation. Our analysis investigates the $\tilde{\nu_\tau} \to e\mu$ decay channel and sets limits on the $\tilde{\nu_\tau}$ mass and on two of its RPV couplings to Standard Model particles, λ_{132} and λ'_{311}. The data represents 344 pb^{-1} of $p\bar{p}$ collisions at $\sqrt{s} = 1.96$ TeV with the CDF detector at Fermilab.

Preliminary Results for Summer 2005 Conferences

1 Introduction

This note describes a search for high mass resonances that decay to an oppositely charged $e\mu$ final state in $\sqrt{s} = 1.96$ TeV $\bar{p}p$ collisions with the CDF detector at the Fermilab Tevatron. We scan an invariant mass range from 50 to 800 GeV/c^2 for an excess of events above the level predicted by the Standard Model. While an $e\mu$ signature is prevalent in many models of new physics, we set limits by interpreting the data in the context of a particular Supersymmeteric model, the R-parity violating (RPV) production and decay of the tau sneutrino. The theoretical cross section for the $d\bar{d} \to \tilde{\nu}_\tau \to e\mu$ process depends on the strength of two couplings in the Supersymmetric Lagrangian, λ_{132} and λ'_{311}. At each mass point in the analysis we consider a range of values for the couplings below currently published limits, $\lambda_{132} = 0.05$ and $\lambda'_{311} = 0.16$ [1]. This allows us to extend an earlier $\tilde{\nu_\tau}$ mass limit set for particular values of the RPV couplings [2], which we use to parameterize the mass limit.

2 Data Sample & Event Selection

The analysis is based on an integrated luminosity of 344 pb^{-1} collected with the CDFII detector between March 2002 and August 2004. The CDF detector is described in detail elsewhere [3]. We use data acquired with two distinct inclusive lepton triggers to construct an $e\mu$ dataset. The inclusive electron trigger selects events with a central electron of $E_T > 18$ GeV and with $| \eta | < 1.1$. Events that pass the inclusive muon trigger contain a muon with track segments in the central muon (CMU) and central muon upgrade (CMP) drift chambers, $| \eta | < 0.6$, or in the central muon extension (CMX) chamber, $0.6 < | \eta | < 1.0$. We require an offline confirmation of both the electron and muon trigger decisions when such muons and electrons pass the event selection criteria described below. We additionally consider two looser categories of muons that are not used by the inclusive muon trigger, those with track segments in the CMU or CMP chambers only. In selected events where the muon is of these categories we require an offline confirmation of the inclusive electron trigger only.

From this inclusive lepton dataset we select events with a reconstructed electron $E_T > 20$ GeV and an oppositely charged muon with $P_T > 20$ GeV/c. The difference between the track Z_0 of the electron and muon is required to be less than 5 cm so that the two are consistent with a common vertex. Both leptons must have isolated energy depositions in the CDF calorimeter and we demand that their reconstructed tracks meet a number of quality requirements.

3 Signal Acceptance

The total acceptance is measured using a combination of data and Monte Carlo. The geometric times kinematic acceptance, α_{gk}, of the basic $e\mu$ event selection is measured with the PYTHIA Monte Carlo program [4]. Events with a reconstructed $e\mu$ pair that pass the selection criteria and with $M_{e\mu}$ falling within

$\pm 1.5\sigma$ of the generated value are accepted. The total acceptance, α_t, is obtained by applying scale factors to α_{gk} that account for differences between data and Monte Carlo. These factors include a set of values used to scale the efficiencies for identifying isolated, high P_T leptons in Monte Carlo to the values measured for data. Other factors correct the acceptance to reflect the efficiency of the trigger selection in data. Figure 1. shows a fit to α_t as a function of the reconstructed $e\mu$ invariant mass.

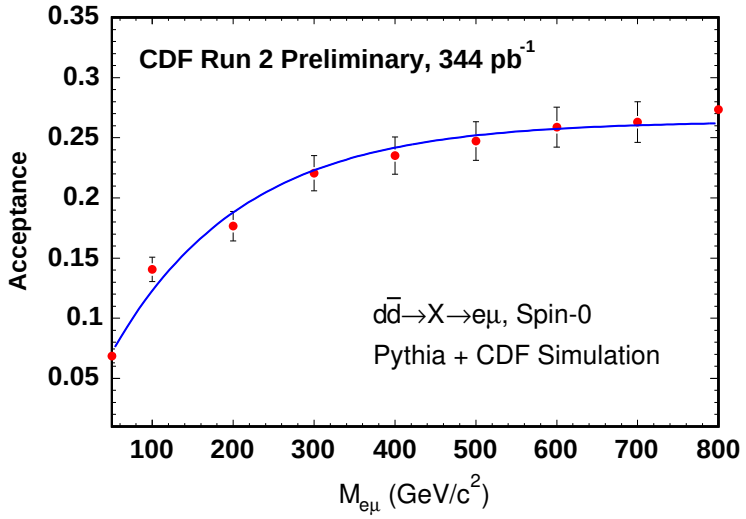

Figure 1: The total acceptance for the $e\mu$ event selection as a function of $e\mu$ invariant mass. The blue line is a fit to the total acceptances calculated for the Monte Carlo signal sample and is used in the evaluation of the observed cross section.

4 Backgrounds

The expected contributions from background over the 50 to 800 GeV/c^2 range are listed in Table 1. The table presents the background predictions divided into two $M_{e\mu}$ ranges, a 50-100 GeV/c^2 'control' and a 100-800 GeV/c^2 'signal' region. The control region has been previously excluded [2] and is used in this study to verify the event selection and accuracy of Monte Carlo predictions. The dominant background in this region is $Z \rightarrow \tau\tau$ where each of the taus decays leptonically. $t\bar{t}$ and WW events constitute the majority of background in the signal region. The amount of background here is small however, and we do not apply optimized kinematic cuts to reduce it further since we seek to maximize signal acceptance.

Channel	Control Region	Signal Region
$Z \to \tau\tau$	$38.77 \pm 0.63 \pm 2.33$	$0.57 \pm 0.01 \pm 0.03$
diboson	$6.63 \pm 0.18 \pm 0.37$	$3.48 \pm 0.10 \pm 0.19$
$t\bar{t}$	$3.57 \pm 0.05 \pm 0.21$	$3.16 \pm 0.05 \pm 0.19$
fake lepton	$2.90 \pm 1.10 \pm 1.33$	$0.44 \pm 0.40 \pm 0.40$
Prediction	$51.87 \pm 1.11 \pm 2.72$	$7.66 \pm 0.41 \pm 0.48$
Observation	56 ± 7.48	5 ± 2.24

Table 1: Expected background in the signal and control regions. The first column shows background predictions and our observation for our control region, 50-100 GeV/c^2. The second column shows results for the 100-800 GeV/c^2 signal region. Data and predictions agree well in both regions.

Estimates shown for Standard Model processes are obtained by applying the $e\mu$ event selection to PYTHIA Monte Carlo samples of the listed physics processes. An additional source of background in the $e\mu$ channel arises from jets that are misidentified as leptons. To estimate the background contribution from this source we measure the probability for a jet to be reconstructed as a lepton using jet-enriched data samples. After removing leptons due to Drell-Yan and leptonic W decays from the samples, those remaining (*fake leptons*) are primarily associated with misidentified jets. We calculate the misidentification probability as the ratio of the number of leptons that pass our full list identification cuts to the number of 'candidate' leptons in the samples that pass a looser subset of the identification criteria. The probabilities are parameterized as functions of electron E_T and muon P_T.

We apply the probabilities to candidate signal lepton+jet events in the inclusive lepton sample to obtain an estimate of the $e\mu$ background from fake leptons. The electron and muon candidates are chosen from events with one lepton of alternate flavor that passes the full list of identification cuts. We next form an invariant mass distribution of the identified and candidate $e\mu$ pair. This distribution is weighted by the misidentification probability corresponding to the candidate electron E_T or muon P_T to provide an estimate of the number of expected $e\mu$ events from fake leptons.

5 Statistical Techniques

We divide the 50 to 800 GeV/c^2 mass range into segments using a fit to the RMS of the reconstructed Monte Carlo mass distributions. Segment size is

determined by 3 times the RMS at the mass on which the segment is centered and consecutive segments are reached by stepping with 1/10th the RMS. We calculate an upper-limit cross section at the 95% C.L. for each segment using events with an $M_{e\mu}$ contained by the segment and the acceptance defined for its central point. The cross section calculation involves a Bayesian routine that accounts for the effect of uncertainties and background on the limit [5].

Before calculating the observed upper-limit cross section for data, we use the Bayesian technique to estimate our sensitivity by assuming an observation at the level of the expected background. We perform a number of pseudo-experiments in which the 'observation' is taken as the sum of the expected background contributions, each Poisson-fluctuated from their Monte Carlo prediction. Figure 3., included in Section 7., displays the resulting average 95% C.L. upper-limit cross section and uncertainty bands together with the next-to-leading order (NLO) theoretical cross section for the λ couplings set to their current limits. The NLO cross section is obtained by applying K-factors to the leading order cross section provided in [6].

6 Systematic Uncertainties

Systematic uncertainties in this analysis come from Monte Carlo modeling of the signal acceptance, knowledge of the lepton ID efficiencies and misidentification rates and the uncertainty on the luminosity. The Bayesian limit setting routine takes as input uncertainties on the number of expected background events and on the product of luminosity times acceptance. We summarize the systematic uncertainties on these quantities for the entire 50-800 GeV/c^2 $M_{e\mu}$ range in Table 2.

$\alpha_t \times L$ Uncertainty Source	Fractional Sys. Uncert.
E & P Resolution	3.2%
PDF's	2.4%
Scale Factors	1.6%
Luminosity	6%
N_{BG} Uncertainty Source	Fractional Sys. Uncert.
Luminosity	5.6%
Fake Probabilities	3.1%

Table 2: Summary of Systematic Uncertainties. This tables shows the relative uncertainties on the two quantiles, acceptance times integrated luminosity and total expected background, input to the Bayesian limit setting routine.

The widths of the $\tilde{\nu}_\tau$ mass distributions are used to determine the size of the acceptance windows applied to data and their uncertainties will influence the upper-limit cross section calculated for each range. Uncertainties in the widths are related to the uncertainties in energy and momentum resolution. We quan-

tify this relationship by first smearing the generator-level energy and momentum distributions with resolution functions to match the reconstructed distributions. We then vary the resolution functions by their uncertainties and measure the effect on signal acceptance. The fractional uncertainty on acceptance due to the uncertainty in resolution is found to be 3.2%,

Uncertainties associated with the CTEQ6 PDF's used in the Monte Carlo modeling of the initial-state $p\bar{p}$ also contribute to the uncertainty in signal acceptance. We estimate their effect following a technique described in [7]. This approach defines a set of 20 eigenvectors of parameters to which the PDF's are sensitive and 40 scale factors corresponding to variations of the parameters in opposing directions. We assess the effect of variations in the parameters on acceptance by applying the scale factors to the acceptance calculated for one eigenvector configuration. The relative acceptance differences due to the scale factors taken in quadrature lead to a 2.4% fractional uncertainty in the acceptance.

Uncertainties are also associated with the scale factors used to relate the lepton ID efficiency in Monte Carlo to the values measured for data. The uncertainties differ across lepton categories and together contribute to a 1.6% relative uncertainty on the signal acceptance.

We consider the two types if uncertainties on the expected background. The largest uncertainty on contributions from Standard Model processes follows from the 6% uncertainty on the integrated luminosity. This leads to a 6% relative uncertainty on the Standard Model background expectation and a 5.6% uncertainty on the overall background. The uncertainty on the contribution from fake leptons results from uncertainties in the jet misidentification probabilities. We measure these using the differences between the values found for different jet samples. The relative differences range from 2% to 60% across electron E_T and muon P_T bins, resulting in a 3.1% relative uncertainty on the total background.

7 Results

Figure 2. shows the $M_{e\mu}$ distributions of data and background Monte Carlo. The data is well described by our background predictions and we find no evidence for RPV sneutrino decay. To quantify their level of agreement, we rebin the data and background distributions shown in 2 and perform a χ^2 test. Before analyzing the data we select variable width mass bins to ensure occupancies sufficient for the test (5 Monte Carlo events per bin). We find a total reduced chi-square statistic of 1.35 a p-value of 23% for the bins, indicating that our results are indeed consistent with the Standard Model.

Figure 3. displays the observed upper-limit cross section, our calculated sensitivity and the theoretical $d\bar{d} \rightarrow \tilde{\nu}_\tau \rightarrow e\mu$ cross section. The displayed theory curve, calculated using the current limits for the λ_{311} and λ'_{132} couplings, intersects the observed cross section near 460 GeV/c^2. This value represents the limit on sneutrino mass we set for the given values of the couplings, 0.05 and 0.16 respectively.

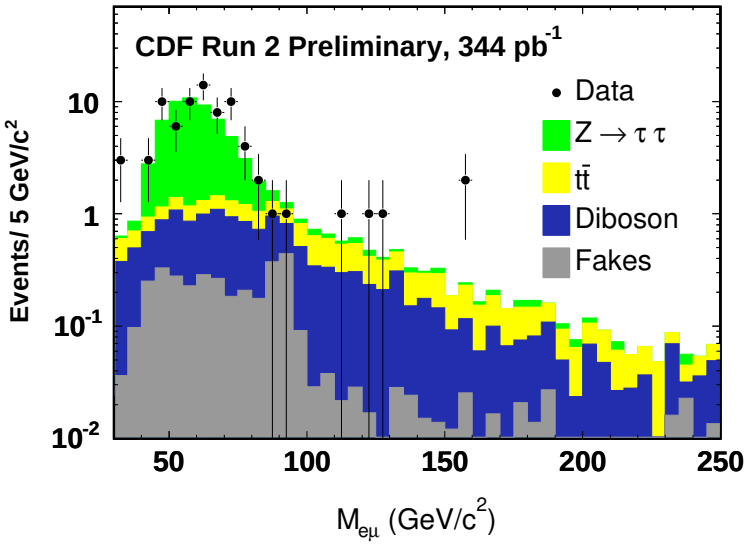

Figure 2: Data and Background Monte Carlo Mass Distributions. This plot shows the invariant mass of reconstructed $e\mu$ pairs in data and the summed distributions of background Monte Carlo predictions. The distributions agree well, despite a few fluctuations in data above 100 GeV/c^2.

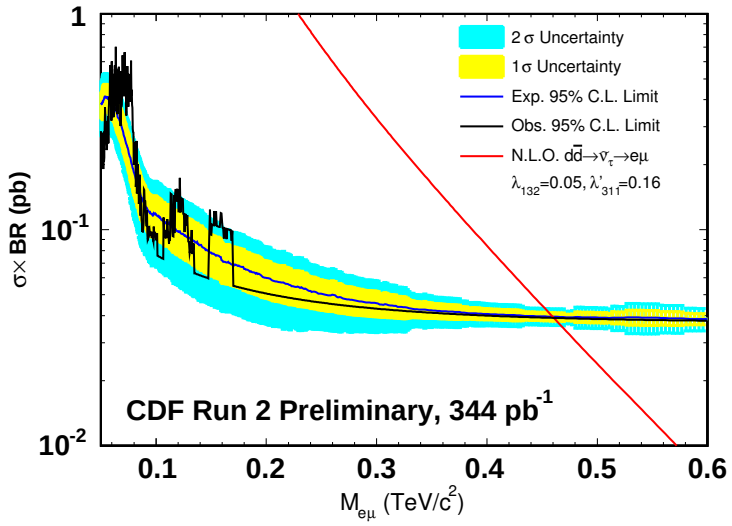

Figure 3: Observed and theoretical sneutrino decay cross section. The upper-limit cross section calculated for data (black) is shown together with the average 95% C.L. sensitivity (blue, with 1σ (yellow) and 2σ (cyan) bands) and theoretical cross section for the current best limits of λ_{132} and λ'_{311}. The intersection of the theoretical cross section and the observed upper-limit near 460 GeV/c^2 represents the $\tilde{\nu_\tau}$ mass limit we set for the chosen values of the couplings.

We construct exclusion regions in the $\lambda(\lambda') - M_{e\mu}$ plane by decreasing the value for each coupling independently to 1/100th of their current limits and finding the intersection of the resulting theory curve with the observed upper-limit cross section. We shown the exclusion constructed for λ'_{311} versus $M_{e\mu}$, parameterized by λ_{132}, in Figure 4.

In conclusion, we've searched for an excess of $e\mu$ events across a 50-800 GeV/c^2 invariant mass range. Our results are consistent with Standard Model predictions and we interpret these in the context of the RPV production and decay of the tau sneutrino. We set limits on the $\tilde{\nu_\tau}$ mass and on two of its couplings to Standard Model particles, λ_{132} and λ'_{311}.

8 Acknowledgments

We thank the Fermilab staff and the technical staffs of the participating institutions for their vital contributions. This work was supported by the U.S. Department of Energy and National Science Foundation; the Italian Istituto Nazionale

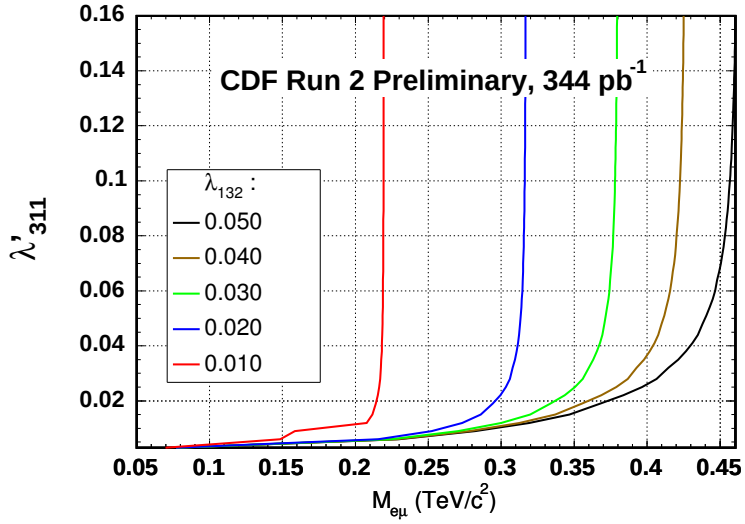

Figure 4: $\lambda - M_{e\mu}$ Exclusion Regions. The curves shown represent the excluded range of $\lambda'_{311} - M_{e\mu}$ for various values of λ_{132}.

di Fisica Nucleare; the Ministry of Education, Culture, Sports, Science and Technology of Japan; the Natural Sciences and Engineering Research Council of Canada; the National Science Council of the Republic of China; the Swiss National Science Foundation; the A.P. Sloan Foundation; the Bundesministerium fuer Bildung und Forschung, Germany; the Korean Science and Engineering Foundation and the Korean Research Foundation; the Particle Physics and Astronomy Research Council and the Royal Society, UK; the Russian Foundation for Basic Research; the Comision Interministerial de Ciencia y Tecnologia, Spain; and in part by the European Community's Human Potential Programme under contract HPRN-CT-20002, Probe for New Physics.

References

[1] Marc Chemtob. hep-ph/0406029, 2 June 2004.

[2] D. Acosta. hep-ex/0307012, 22 October 2003.

[3] F. Abe, et al., Nucl. Instrum. Methods Phys. Res. A **271**, 387 (1988); D. Amidei, et al., Nucl. Instum. Methods Phys. Res. A **350**, 73 (1994); F. Abe, et al., Phys. Rev. D **52**, 4784 (1995); P. Azzi, et al., Nucl. Instrum.

Methods Phys. Res. A **360**, 137 (1995); The CDFII Detector Technical Design Report, Fermilab-Pub-96/390-E

[4] T. Sjostrand et al., High-Energy-Physics Event Generation with PYTHIA 6.1, Comput. Phys. Commun. **135**, 238 (2001).

[5] Joel Heinrich, Craig Blocker, John Conway, Luc Demortier, Louis Lyons, Giovanni Punzi, Pekka K, Sinervo. "Interval estimation in the presence of nuisance parameters. 1. Bayesian approach". (2004).

[6] S. Dimopolous. R. Esmailzadeh. L.J. Hall. J.P. Merlo and G. D. Starkman. Phys Rev. D. **41.** 2099 (1990)

[7] J. Pumplin, D.R. Stump, J. Huston, H.L. Lai, P. Nadolsky, W.K. Tung. hep-ph/0201195, 3 Feburary 2003.